Discrimination of rice panicles by hyperspectral reflectance data based on principal component analysis and support vector classification[*]

Zhan-yu LIU[†1,2,3], Jing-jing SHI[1], Li-wen ZHANG[1], Jing-feng HUANG[†‡1,2,3]

(*[1]Institute of Agricultural Remote Sensing and Information System Application, Zhejiang University, Hangzhou 310029, China*)
(*[2]Ministry of Education Key Laboratory of Environmental Remediation and Ecological Health, Zhejiang University, Hangzhou 310029, China*)
(*[3]Key Laboratory of Agricultural Remote Sensing and Information System in Zhejiang Province, Hangzhou 310029, China*)
[†]E-mail: zdrsbond@zju.edu.cn; hjf@zju.edu.cn
Received July 6, 2009; Revision accepted Nov. 16, 2009; Crosschecked Nov. 19, 2009

Abstract: Detection of crop health conditions plays an important role in making control strategies of crop disease and insect damage and gaining high-quality production at late growth stages. In this study, hyperspectral reflectance of rice panicles was measured at the visible and near-infrared regions. The panicles were divided into three groups according to health conditions: healthy panicles, empty panicles caused by *Nilaparvata lugens* Stål, and panicles infected with *Ustilaginoidea virens*. Low order derivative spectra, namely, the first and second orders, were obtained using different techniques. Principal component analysis (PCA) was performed to obtain the principal component spectra (PCS) of the foregoing derivative and raw spectra to reduce the reflectance spectral dimension. Support vector classification (SVC) was employed to discriminate the healthy, empty, and infected panicles, with the front three PCS as the independent variables. The overall accuracy and kappa coefficient were used to assess the classification accuracy of SVC. The overall accuracies of SVC with PCS derived from the raw, first, and second reflectance spectra for the testing dataset were 96.55%, 99.14%, and 96.55%, and the kappa coefficients were 94.81%, 98.71%, and 94.82%, respectively. Our results demonstrated that it is feasible to use visible and near-infrared spectroscopy to discriminate health conditions of rice panicles.

Key words: Rice panicle, Principal component analysis (PCA), Support vector classification (SVC), Hyperspectral reflectance, Derivative spectra

doi:10.1631/jzus.B0900193   **Document code:** A   **CLC number:** TP7; S43

1 Introduction

With rapid increase of human population, there is a fast growth of food consumption worldwide. To increase crop production, it is important to control insect and disease in agriculture (Karimi *et al.*, 2006). An accurate assessment of pest distribution and damage caused by insect and disease is needed in order to implement near real-time strategies of control and protection (Pedigo, 1995). Currently, the most commonly used method of agricultural pest detection is visual evaluation (Horst *et al.*, 1984; Nilsson, 1995; Richardson *et al.*, 2001; Steddom *et al.*, 2005), but the limitation of this technique is time-consuming and labor-intensive if it is implemented over a wide range (Kobayashi *et al.*, 2001). Remote sensing techniques from ground to satellite platform have proven to be very effective to monitor insect infestation and disease epidemic in agricultural crops and other plants within a given growth condition (Mirik *et al.*, 2006).

Many studies have shown that the basis for distinguishing healthy and stressed plants using optical

---

remote sensing technique is their differences in reflectance in different spectral regions. Healthy plant often has a high reflectance in the near-infrared (NIR) region determined by cellular and subcellular structures and a low visible reflectance due to strong pigment absorption (Knipling, 1970; Riedell and Blackmer, 1999). Changes in pigment concentrations as well as internal leaf structure are strongly related to the physiological status, and consequently, spectral features of plant (Blackburn, 1998a; 1998b; Mirik *et al*., 2007). The current investigations suggested that stressed plants have a lower reflectance in NIR region (700–1300 nm), a higher reflectance in the far-red region of the spectrum, and a consequent shift of the red edge (Cibula and Carter, 1992; Carter, 1993; Malthus and Madeira, 1993; Shibayama *et al*., 1993). In addition to reflectance, numerous studies have documented the use of vegetation indices such as ratio vegetation index (RVI) and normalized difference vegetation index (NDVI) in the detection of crop stress (Kobayashi *et al*., 2001; Vigier *et al*., 2004; Yang *et al*., 2009). Furthermore, various statistical and artificial intelligence methods have been used to analyze the remotely sensed data in agricultural crops. Among many, popular approaches include cluster analysis (Holden and LeDrew, 1998), principal component analysis (PCA) (Zhang *et al*., 2002; 2003), partial-least square (PLS) regression (Huang and Apan, 2006), artificial neural networks (ANN) (Liu *et al*., 2008), and support vector machine (SVM) (Shi *et al*., 2009), and so forth.

Although at the leaf and canopy level there has been some progress on remote sensing studies about insect and disease outbreaks in rice including leaf folder (Shi *et al*., 2009), panicle blast (Kobayashi *et al*., 2001), leaf blast (Wu *et al*., 2002), leaf brown spot (Liu *et al*., 2007; 2008), and sheath blight (Qin *et al*., 2003; Qin and Zhang, 2005), hardly any study was found to differentiate stressed panicles of rice crop due to insect and pathogen using remote sensing techniques. Rice brown planthopper (*Nilaparvata lugens* Stål), which is one of the most destructive insects in rice throughout the world, primarily feeds on the leaf sheaths and stems at the basal portion of the rice plant and sucks the phloem sap. Eventually the whole plant turns brown and dies, and the grains of rice become empty, thus being called empty panicles (Sōgawa, 1982). About 25 million hectares of

rice were damaged due to the rice brown planthopper, accounting for a 2.77 million-ton loss in rice production in 2005 only (Wang *et al*., 2008). Rice false smut (RFS) is one of most devastating diseases of rice grain infected by the fungus *Ustilaginoidea virens* in most of the major rice-growing areas. Toxin produced by *U. virens* is noxious to human being and livestock, and results in yield loss of rice as well (Ou, 1985).

The overall aim of this study was to examine the capability of the support vector classification (SVC) method in discriminating the different health status of rice panicles. The specific goals were to (1) examine the response characteristics of the raw and derivative spectra of empty panicles caused by rice brown planthopper and infected panicles caused by rice false smut disease; (2) select the principal component spectra (PCS) derived from the raw and derivative spectra to see whether selected PCS could reliably represent the health status of rice panicles; and (3) discriminate the empty and infected panicles from healthy panicles with the aforementioned features using SVC method.

2 Materials and methods

2.1 Study sites and materials

The samples of empty rice panicles caused by rice brown planthopper (*Nilaparvata lugens* Stål) were collected in the experimental farmland of Zhejiang University (30°14′ N, 120°10′ E), Zhejiang Province, China, on Oct. 7 and 17, 2008. On each day, an equal number of 36 panicles of rice cultivar, Xiushui 110, were collected.

The samples of healthy panicles and infected panicles caused by rice false smut (*U. virens*) were collected from two rice fields. The first field is located near Sankengkou village (28°42′ N, 119°44′ E), Wuyi county, Zhejiang, and the second field at the Agronomy Research Center, Ningbo Academy of Agricultural Sciences (29°50′ N, 121°37′ E), Yinzhou district, Zhejiang on Oct. 8 and 25, 2008. On each day and in the each field, 40 (total 160) panicles of rice cultivars, Jingdao 4 or A10/F5006, were collected.

2.2 Measurements of panicle hyperspectra

The healthy, empty, and infected panicles, which were verified by a phytopathologist, were cut from

the rice individuals in the paddy field, and then the samples were put into an incubator with ice block in order to prevent water loss. Then these samples were transported to the laboratory for hyperspectral measurement. Rice panicle hyperspectral reflectance was measured with a portable spectrophotometer (ASD FieldSpec® Pro FR, Analytical Spectral Devices Inc., Boulder, CO, USA) over the 350 to 2500 nm wavelength range coupled with an integrating sphere (Model LI-1800, LI-COR Inc., Lincoln, NE, USA).

2.3 Data preprocessing

Due to severe instrument and system noise, hyperspectral reflectance at more than 1000 nm wavelengths was ineffective and not used in further analysis. In addition, hyperspectral reflectance was smoothed with a seven-step moving average to suppress the instrumental and environmental noise before these data were further analyzed (Kobayashi *et al.*, 2001). In order to analyze the data conveniently, the total dataset was divided into two parts. The training dataset included the empty panicles (collected on Oct. 7, 2008), and healthy and infected panicles (collected on Oct. 8, 2008). The testing dataset included the remaining samples of rice panicles collected on Oct. 17 and 25, 2008.

Derivative spectroscopy virtually uses the changes of spectral reflectance or radiance with respect to wavelength to sharpen spectral features (Rundquist *et al.*, 1996; Holden and LeDrew, 1998). Application of this technique is proposed to tackle analogous problems such as background signals and to solve overlapping problems in spectral features. The simplest method of finding derivatives in practice is by dividing the difference between successive spectral reflectance by the wavelength interval separating them (Demetriades-Shah *et al.*, 1990). The first-order and second-order derivative reflectance (FDR and SDR) spectra were calculated by this method in our study. The former, FDR, provides slope information on the rate of change reflectance with respect to wavelength, while the latter, SDR, reveals the change in slope with respect to wavelength (Holden and LeDrew, 1998).

2.4 Analytical techniques

PCA has been used as a data compression technique for preserving the total variance in the transfor-

mation and minimizing the mean square approximate errors (Ingebritsen and Lyon, 1985). Uncorrelated linearly transformed components are derived from the original dataset such that the first principal component accounts for the maximum possible proportion of the variance of the original dataset, and subsequent components account for the maximum proportion of the unexplained residual variance, and so on (Fung and LeDrew, 1987). This technique is very suitable for hyperspectra data for high dependence and autocorrelation in adjacent wavebands (Panda *et al.*, 2009).

SVC is one of the most important parts of support vector machine (SVM) and a popular technique for data classification. The aim of SVC is to devise a computationally efficient way of learning 'good' separating hyperplanes in a high dimensional feature space based on the generalization and optimization theories; the former gives clear guidance about how to control capacity and hence prevent overfitting by controlling the hyperplane margin measures, while the latter provides the mathematical techniques necessary to find hyperplanes optimizing these measures (Cristianini and Shawe-Taylor, 2000). In this study, SVC was run in LIBSVM (Library for Support Vector Machines) developed by Chang and Lin (2001). LIBSVM is a library for SVM, and its goal is to help users to easily use SVM as a tool. LIBSVM includes C-SVC, v-SVC, distribution estimation (one-class SVM), and other models. C-SVC belongs to nonlinear soft separation classification for solving binary and multicategory problems and it was adopted in our research. In LIBSVM, the key parameters such as kernel function γ, penalty parameter C and other parameters are provided with default selections available.

Kappa coefficient (viz. KHAT statistic), which is one measure of the level of agreement, has been applied to compare and address the best results from different classification approaches for the remotely sensed data (Congalton, 1991). A kappa coefficient of 1 denotes a full agreement and 0 denotes full disagreement between the actual and predicted values (Abalos *et al.*, 2000; Kitchen *et al.*, 2005). In this study, overall accuracy as well as kappa coefficient was chosen to evaluate the accuracy of C-SVC for different spectra types such as raw, first and second derivative reflectance spectra.

3 Results

3.1 Spectral reflectance characteristics of rice panicles

The spectral response of rice panicles to biotic stress such as insect or fungi (Fig. 1) provided a theory basis for applying visible and NIR spectroscopy to crop pest management and harvesting machinery design. The raw spectral response characteristic of healthy rice panicle was like the green leaf in the visible and NIR regions because there were much larger amounts of pigment such as chlorophyll and carotenoid in heath panicles than in empty and infected ones (Fig. 1a). The rice planthopper fed on the juice in rice sheath and stem and led to empty panicle, so empty panicle was drier compared with healthy panicle (Sōgawa, 1982). Then raw reflectance spectra curve of empty panicle was approximately linear. The fungus *U. virens* transforms individual grains of the panicle into yellowish-green or greenish-black spore balls of a velvety appearance (Ou, 1985). Reflectance of infected rice panicle decreased by 65.97% and 52.04% in the visible and NIR regions, respectively. This was probably due to lower pigment contents and compact arrangement structure, respectively.

Spectral derivative analysis was performed to more closely examine the spectral differences in reflectance at specific wavelengths (Holden and LeDrew, 1998). The amplitude of the FDR for healthy panicle was bigger than those of empty and infected ones (Fig. 1b). The peak waveband of healthy panicle in the blue-green region was located at 518 nm, but the peak wavebands of empty and infected panicles shifted toward the short wavebands about 17 and 10 nm, respectively. The red edge is the sharp change in the FDR spectra between 680 and 750 nm and has been defined as the point of the maximum slope, which was defined as the indicator of plant stress (Horler *et al*., 1983). The red edge of healthy panicle was at 696 nm, while that of empty panicle at 692 nm. There were double peaks at 696 and 735 nm for the infected panicle.

There existed much noise for the SDR in the spectral regions less than 500 nm and more than 800 nm, especially for empty panicle shown in Fig. 1c. The amplitude of SDR for healthy panicle was 5 and 7 times bigger than those of empty and infected panicles, respectively. The peak wavebands in the far-red region for the empty, healthy, and infected panicles were 682, 685 and 686 nm, respectively. In addition, for SDR the difference between empty and infected panicles was smaller than that for FDR.
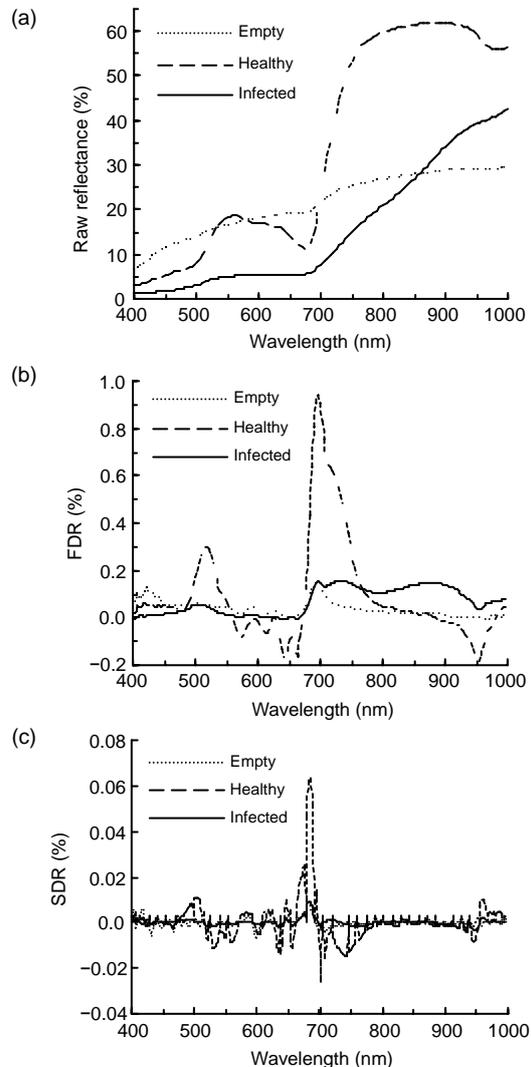

Fig. 1 Spectral reflectance properties of rice panicles under laboratory conditions. (a) Raw reflectance spectra; (b) First-order derivative reflectance (FDR) spectra; (c) Second-order derivative reflectance (SDR) spectra

3.2 Principal component analysis

The results of the PCA revealed that the cumulative contributions of the front three components for raw, FDR and SDR spectra were 99.8%, 99.2% and 85.5%, respectively (Table 1). Generally, when the cumulative contribution of the front several components is more than 80%~85%, the remaining

components can be omitted in further analysis (Wang, 1999). And then the front three components could be regarded as the PCS in our study.

Taking the raw spectra as an example, the majority of samples for the empty, healthy, and infected panicles were clustered with the front three PCS as shown in Fig. 2. The scores of all the infected panicles for the principal component 1 (PC1) and PC2 were negative. The scores of the whole empty panicles were negative for PC1, but positive for PC2. The scores of most healthy panicles for PC1 and PC2 were just reverse to empty panicles. The scores of infected, empty, and healthy panicles for PC3 appeared irregularly in comparison with PC1 and PC2 and such result indicated that PC3 contained little spectra information (Table 1). Overall, the cluster results of rice panicles under different health conditions were basically satisfactory. However, visual recognition was needed to make clusters for rice panicles with PCS.

3.3 Results of support vector classification

In order to make up for the disadvantage of PCA in clusters, the method of SVC was used to automatically distinguish the different health con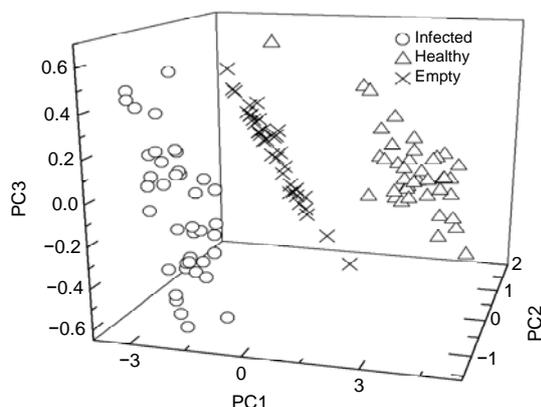ditions of rice panicles. For the purpose of this study, the dataset was divided into two parts. The training dataset was used to build the classification model for calibration purpose, and the testing dataset for validation purpose.

The SVC model was calibrated using the training dataset containing the dependent (i.e., panicle classification) and independent (i.e., the front three PCS) variables. In order to obtain the optimum classification result, the model was run repeatedly with different sets of values of γ and C at least three times for cross-validation. When kernel function γ was radial basis function (RBF) and penalty parameter C was 1, SVC model was able to completely classify different categories of rice panicles and the optimum results for the testing dataset are presented in Table 2.

For all the three categories the classification results for different spectral types were good, and the misclassified categories were small. In the case of empty panicles, the SVC model with FDR and SDR spectra could fully differentiate them from healthy and infected panicles, but worse result was gained for the SVC model with raw spectra. Whatever spectral types, the SVC model could completely discriminate the infected panicles. The SVC model with raw spectra could perfectly distinguish the healthy panicles from empty and infected ones; however, FDR and SDR models failed to produce similar results (Table 2). Overall accuracies of 96.55%, 99.14%, and 96.55% were obtained with the testing dataset for the raw, FDR, and SDR spectra, respectively (Table 3). To examine the level of agreement between actual and classified categories, the kappa coefficient was also calculated (Table 3). The high values of kappa coefficients (94.81%, 98.71%, and 94.82% for raw, FDR and SDR spectra, respectively) indicated good model performance of SVC and strong agreement between the actual and classified categories. On the whole, the SVC model had the best classification result with the front three PCS derived from FDR spectra.

Fig. 2 Score plot of the training dataset on the front three principal components of raw spectra

Table 1 Percentage of explained variance for the front three PCS

Spectral type	Explained variance (%)							
	Training dataset				Testing dataset			
	PC1	PC2	PC3	Total	PC1	PC2	PC3	Total
Raw	85.7	13.3	0.8	99.8	78.5	19.9	1.3	99.7
FDR	94.2	4.0	1.0	99.2	75.7	20.9	3.0	99.6
SDR	71.8	9.8	3.9	85.5	87.3	6.3	1.3	94.9

Table 2 Error matrix for C-SVC from the testing dataset with PCS derived from three spectral types

Actual	Classified											
	Raw				FDR				SDR			
	Empty	Infected	Healthy	Sum	Empty	Infected	Healthy	Sum	Empty	Infected	Healthy	Sum
Empty	32	0	4	36	36	0	0	36	36	0	0	36
Infected	0	40	0	40	0	40	0	40	0	40	0	40
Healthy	0	0	40	40	0	1	39	40	1	3	36	40
Sum	32	40	44	116	36	41	39	116	37	43	36	116

Table 3 Comparison of the two accuracy measures for the three spectral types

Type	Overall accuracy (%)	Kappa coefficient (%)
Raw	96.55	94.81
FDR	99.14	98.71
SDR	96.55	94.82

4 Discussion and conclusion

In the present study, the raw reflectance of rice empty panicles was found higher than that of healthy panicles in the visible region (400–695 nm) except the green peak (531–577 nm), and lower than that in the whole NIR region (Fig. 1). The raw reflectance of infected panicles was lower than that of healthy panicles in all the visible and NIR regions. Obviously our result was not completely consistent with previous studies (Carter, 1993; Riedell and Blackmer, 1999). In addition, the FDR and SDR spectra were analyzed. The blue edge positions for empty and infected panicles shifted toward short wavebands over 10 nm compared with healthy panicles, and too much noise for SDR was detected in the blue-green and NIR regions (<500 nm, >800 nm). All these results are in agreement with Liu et al. (2007; 2008). However, the FDR had two peaks in red edge region for infected panicles and shifted toward short wavebands by about 4 nm for empty panicles, which differed from Liu et al. (2007; 2008).

The front several PCS were usually sensitive to the reflectance spectra of healthy and stressed plants and their linear combinations in previous and current researches (Holden and LeDrew, 1998), and similar results were obtained in our study. The information variations, not only from the training dataset, but also from the testing dataset, explained by the front three PCS derived from the raw, FDR and SDR spectra, were found more than 85% in the present study (Table 1). Furthermore, the cluster analysis for PCS was inconvenient for visual interpretation (Fig. 2), which is coincident with Panda et al. (2009).

The combination of SVC and PCA would give rise to satisfactory classification results. The optimum results were obtained with kernel function γ of RBF and penalty parameter C of 1 after repeated running at least for three times (Table 2). The SVC model coupling with the front three PCS derived from FDR had the best performance than those from raw and SDR spectra in classification of rice panicles (Table 3), and the overall accuracy and kappa coefficient were 99.14% and 98.71%, respectively. The value of overall accuracy was higher than kappa coefficient; identical conclusion was obtained by Karimi et al. (2006).

We demonstrated the feasibility of using visible and NIR spectroscopy to discriminate the health status of rice panicles under the laboratory condition. However, the canopy architecture of agricultural crops is very complex under field conditions. More external factors (e.g., illumination, cloudy shadow, and shallow water in the paddy field) coexist at the canopy level (Liu et al., 2007; 2008), which consequentially bring about much more noise in hyperspectral reflectance and lower classification accuracy for stressed crops and their organs. Otherwise, the spectra analysis is far from remote sensing of crop disease detection using airborne or satellite data. Moreover, the infected crops in the field are always in a small proportion to a whole field. And this small proportion is usually not enough for remote detection of the disease from the airborne or satellite images if the spatial resolution is not very high. Therefore, further studies should address how to extrapolate the current research using ground-based remote sensing techniques to airborne or spaceborne platforms.

5 Acknowledgement

References

Abalos, P., Daffner, J., Pinochet, L., 2000. Evaluation of three *Brucella* soluble antigens used in an indirect ELISA to discriminate S19 vaccinated from naturally infected cattle. *Veterinary Microbiology*, **71**(1-2):161-167. [doi:10.1016/S0378-1135(99)00141-8]

Blackburn, G.A., 1998a. Quantifying chlorophylls and carotenoids at leaf and canopy scales: an evaluation of some hyperspectral approaches. *Remote Sensing of Environment*, **66**(3):273-285. [doi:10.1016/S0034-4257(98)00059-5]

Blackburn, G.A., 1998b. Spectral indices for estimating photosynthetic pigment concentrations: a test using senescent tree leaves. *International Journal of Remote Sensing*, **19**(4):657-675. [doi:10.1080/014311698215919]

Carter, G.A., 1993. Responses of leaf spectral reflectance to plant stress. *American Journal of Botany*, **80**(3):239-243. [doi:10.2307/2445346]

Chang, C.C., Lin, C.J., 2001. LIBSVM: A Library for Support Vector Machines. Software available from http://www.csie.ntu.edu.tw/~cjlin/libsvm

Cibula, W.G., Carter, G.A., 1992. Identification of a far-red reflectance response to ectomycorrhizae in slash pine. *International Journal of Remote Sensing*, **13**(5):925-932. [doi:10.1080/01431169208904165]

Congalton, R.G., 1991. A review of assessing the accuracy of classification of remotely sensed data. *Remote Sensing of Environment*, **37**(1):35-46. [doi:10.1016/0034-4257(91)90048-B]

Cristianini, N., Shawe-Taylor, J., 2000. An Introduction to Support Vector Machines and Other Kernel-Based Learning Methods. Cambridge University Press, London, UK, p.93-112.

Demetriades-Shah, T., Steven, M., Clark, J., 1990. High-resolution derivative spectra in remote sensing. *Remote Sensing of Environment*, **33**(1):55-64. [doi:10.1016/0034-4257(90)90055-Q]

Fung, T., LeDrew, E., 1987. Application of principal component analysis to change detection. *Photogrammetric Engineering and Remote Sensing*, **53**(12):1649-1658.

Holden, H., LeDrew, E., 1998. Spectral discrimination of healthy and non-healthy corals based on cluster analysis, principal component analysis, and derivative spectroscopy. *Remote Sensing of Environment*, **65**(2):217-224. [doi:10.1016/S0034-4257(98)00029-7]

Horler, D.N.H., Dockray, M., Barber, J., 1983. The red edge of plant leaf reflectance. *International Journal of Remote Sensing*, **4**(2):273-288. [doi:10.1080/01431168308948546]

Horst, G.L., Engelke, M.C., Meyers, W., 1984. Assessment of visual evaluation techniques. *Agronomy Journal*, **76**(4): 619-622.

Huang, J.F., Apan, A., 2006. Detection of *Sclerotinia* rots disease on celery using hyperspectal data and partial least squares regression. *Journal of Spatial Science*, **52**(1): 131-144.

Ingebritsen, S.E., Lyon, R.J.P., 1985. Principal component analysis of multitemporal image pairs. *International Journal of Remote Sensing*, **6**(5):687-696. [doi:10.1080/01431168508948491]

Karimi, Y., Prasher, S.O., Patel, R.M., Kim, S.H., 2006. Application of support vector machine technology for weed and nitrogen stress detection in corn. *Computers and Electronics in Agriculture*, **51**(1-2):99-109. [doi:10.1016/j.compag.2005.12.001]

Kitchen, N.R., Sudduth, K.A., Myers, D.B., Drummond, S.T., Hong, S.Y., 2005. Delineating productivity zones on claypan soil fields using apparent soil electrical conductivity. *Computers and Electronics in Agriculture*, **46**(1-3): 285-308. [doi:10.1016/j.compag.2004.11.012]

Knipling, E.B., 1970. Physical and physiological basis for the reflectance of visible and near-infrared radiation from vegetation. *Remote Sensing of Environment*, **1**(3):155-159. [doi:10.1016/S0034-4257(70)80021-9]

Kobayashi, T., Kanda, E., Kitada, K., Ishiguro, K., Torigoe, Y., 2001. Detection of rice panicle blast with multispectral radiometer and the potential of using airborne multispectral scanners. *Phytopathology*, **91**(3):316-323. [doi:10.1094/PHYTO.2001.91.3.316]

Liu, Z.Y., Huang, J.F., Shi, J.J., Tao, R.X., Zhou, W., Zhang, L.L., 2007. Characterizing and estimating rice brown spot disease severity using stepwise regression, principal component regression and partial least-square regression. *Journal of Zhejiang University-SCIENCE B*, **8**(10):738-744. [doi:10.1631/jzus.2007.B0738]

Liu, Z.Y., Huang, J.F., Tao, R.X., Zhang, H.Z., 2008. Estimating rice brown spot disease severity based on principal component analysis and radial basis function neural network. *Spectroscopy and Spectral Analysis*, **28**(9): 2156-2160 (in Chinese).

Malthus, T.J., Madeira, A.C., 1993. High-resolution spectroradiometry: spectral reflectance of field beans leaves infected by *Botrytis* fabae. *Remote Sensing of Environment*, **45**(1):107-116. [doi:10.1016/0034-4257(93)90086-D]

Mirik, M., Michels, G.J.Jr., Kassymzhanova-Mirik, S., Elliott, N.C., Catana, V., Jones, D.B., Bowling, R., 2006. Using digital image analysis and spectral reflectance data to quantify damage by greenbug (Hemitera: Aphididae) in winter wheat. *Computers and Electronics in Agriculture*, **51**(1-2):86-98. [doi:10.1016/j.compag.2005.11.004]

Mirik, M., Michels, G.J.Jr., Kassymzhanova-Mirik, S., Elliott, N.C., 2007. Reflectance characteristics of Russian wheat aphid (Hemiptera: Aphididae) stress and abundance in winter wheat. *Computers and Electronics in Agriculture*,

57(2):123-134. [doi:10.1016/j.compag.2007.03.002]

Nilsson, H.E., 1995. Remote sensing and image analysis in plant pathology. *Annual Review of Phytopathology*, **33**(1): 489-527. [doi:10.1146/annurev.py.33.090195.002421]

Ou, S.H., 1985. Rice Diseases, 2nd Ed. Commonwealth Mycological Institute, Ferry Lane, Kew, Surrey, UK, p.307-311.

Panda, S.S., Hoogenboom, G., Paz, J., 2009. Distinguishing blueberry bushes from mixed vegetation land use using high resolution satellite imagery and geospatial techniques. *Computers and Electronics in Agriculture*, **67**(1-2):51-58. [doi:10.1016/j.compag.2009.02.007]

Pedigo, L.P., 1995. Closing the gap between IPM theory and practice. *Journal of Agricultural Entomology*, **12**(4): 171-181.

Qin, Z., Zhang, M., 2005. Detection of rice sheath blight for in-season disease management using multispectral remote sensing. *International Journal of Applied Earth Observation and Geoinformation*, **7**(2):115-128. [doi:10.1016/j.jag.2005.03.004]

Qin, Z., Zhang, M., Christensen, T., Li, W.J., Tang, H., 2003. Remote Sensing Analysis of Rice Disease Stresses for Farm Pest Management Using Wide-Band Airborne Data. The 23rd International Geoscience and Remote Sensing Symposium, Toulouse, France. IEEE, New York, USA, p.2215-2217.

Richardson, M.D., Karcher, D.E., Purcell, L.C., 2001. Quantifying turfgrass cover using digital image analysis. *Crop Science*, **41**(6):1884-1888.

Riedell, W.E., Blackmer, T.M., 1999. Leaf reflectance spectra of cereal aphid-damaged wheat. *Crop Science*, **39**(6): 1835-1840.

Rundquist, D., Han, L., Schalles, J., Peake, J., 1996. Remote measurement of algal chlorophyll in surface waters: the case for the first derivative of reflectance near 690 nm. *Photogrammetric Engineering and Remote Sensing*, **62**(2):195-200.

Shi, J.J., Liu, Z.Y., Zhang, L.L., Zhou, W., Huang, J.F., 2009. Hyperspectral recognition of rice damaged by rice leaf roller based on support vector machine. *Rice Science*, **23**(3):331-334 (in Chinese).

Shibayama, M., Takahashi, W., Morinaga, S., Akiyama, T., 1993. Canopy water deficit detection in paddy rice using a high-resolution field spectroradiometer. *Remote Sensing of Environment*, **45**(2):117-126. [doi:10.1016/0034-4257 (93)90036-W]

Sōgawa, K., 1982. The rice brown planthopper: feeding physiology and host plant interactions. *Annual Review of Entomology*, **27**(1):49-73. [doi:10.1146/annurev.en.27.01 0182.000405]

Steddom, K., Bredehoeft, M.W., Khan, M., Rush, C.M., 2005. Comparison of visual and multispectral radiometric disease evaluations of cercospora leaf spot of sugar beet. *Plant Disease*, **89**(2):153-158. [doi:10.1094/PD-89-0153]

Vigier, B.J., Pattey, E., Strachan, I.B., 2004. Narrowband vegetation indexes and detection of disease damage in soybeans. *IEEE Geoscience and Remote Sensing Letters*, **1**(4):255-259. [doi:10.1109/LGRS.2004.833776]

Wang, H.W., 1999. Partial Least Squares Regression Method and Applications. National Defense Industry Press, Beijing, China, p.1-274 (in Chinese).

Wang, J.H., Zhao, C.J., Huang, W.J., 2008. Application and Basis of Quantitative Remote Sensing in Agriculture. Science Press, Beijing, China, p.356 (in Chinese).

Wu, S.W., Wang, R.C., Chen, X.B., Shen, Z.Q., Shi, Z., 2002. Effects of rice leaf blast on spectrum reflectance of rice. *Journal of Shanghai Jiaotong University (Agricultural Science)*, **20**(1):73-77 (in Chinese).

Yang, Z., Rao, M.N., Elliott, N.C., Kindler, S.D., Popham, T.W., 2009. Differentiating stress induced by greenbugs and Russian wheat aphids in wheat using remote sensing. *Computers and Electronics in Agriculture*, **67**(1-2):64-70. [doi:10.1016/j.compag.2009.03.003]

Zhang, M., Liu, X., O'Neill, M., 2002. Spectral discrimination of *Phytophthora infestans* infection on tomatoes based on principal component and cluster analysis. *International Journal of Remote Sensing*, **23**(6):1095-1107. [doi:10. 1080/01431160110106078]

Zhang, M., Qin, Z., Liu, X., Ustin, S.L., 2003. Detection of stress in tomatoes induced by late blight disease in California, USA, using hyperspectral remote sensing. *International Journal of Applied Earth Observation and Geoinformation*, **4**(4):295-310. [doi:10.1016/S0303-2434 (03)00008-4]